Compact monolithic SLM 3D-printed filters using pole-generating resonant irises

Qian, Lu; Martinez, Rafael; Salek, Milan; Attallah, Moataz; Wang, Yi; Lancaster, Michael J.

DOI:
10.23919/EuMC50147.2022.9784337

Compact Monolithic SLM 3D-Printed Filters using Pole-Generating Resonant Irises

Lu Qian#1, Rafael Martinez *2, Milan Salek#3, Moataz Attallah*4, Yi Wang#5, Michael J. Lancaster#6

#School of Electronic, Electrical, and Systems Engineering, University of Birmingham, UK

*School of Metallurgy and Materials, University of Birmingham, UK

{1LXQ961}@student.bham.ac.uk, {2R.A.Martinezramos, 3M.Salek, 4M.M.Attallah 5Y.Wang.1, 6M.J.Lancaster}@bham.ac.uk

***Abstract* — This paper proposes a new pole-generating resonant iris structure for the design of iris-coupled cavity filters. By replacing the conventional reactive iris with a resonant iris, extra transmission pole can be generated without increasing the number of resonant cavities. This leads to several design advantages: (i) a more compact filter structure; and (ii) ability to realize wide bandwidth and to improve out-of-band rejection. To demonstrate these, a third-order Chebyshev filter is designed and implemented, occupying the same footprint as a second-order filter. To facilitate the formation of the intricate resonant iris structures, the filter was printed monolithically using selective laser melting (SLM) technique. Very good agreement between the measurements and simulations has been achieved.**

***Keywords* — 3D printing, waveguide filters, wideband, resonant iris.**

I. Introduction

Waveguide coupled cavity filters have been widely used in satellite and base station applications because of their excellent performance in terms of low loss and high-power handling capacity. Recently, the rapid development of wideband communication and carrier aggregation has spurred the growing research activity in wideband waveguide filters [1], [2].

For waveguide filters, there are two typical ways to realize wideband filtering performance. The first one uses coupled single-mode resonators [3]–[5]. However, the increasing size and mass is a well-known drawback as the order of waveguide filter rises. Wider bandwidth requires stronger coupling. The irises which enable strong coupling coefficients are often associated with the degradation of out-of-band performance due to the higher-order modes and iris resonances [6]. Another approach is to use multimode resonator technology [1], [7]. Although this method is well-established for miniature cavity filter, it is often difficult to extend to high-order filters because of the complicated coupling scheme. Filters with multimode resonators are also more sensitive to manufacturing tolerances and often suffer from poor temperature stability [8].

In this paper, a novel pole-generating resonant iris structure is proposed for coupled cavity filters. By substituting the conventional reactive irises with the resonant irises, an extra transmission pole (TP) can be implemented within the space previously occupied by the traditional iris. Meanwhile, stronger coupling can be more readily achieved using this structure, rendering wideband capability. All these features potentially allow a higher-order and wideband filter without excessive size increase.

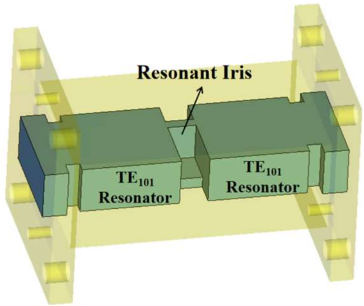

Fig. 1. Internal structures of a third order cavity filter based on the proposed pole-generating resonant iris.

Previously, coupling irises have been modified for new or enhanced functionalities in filters. For instance, irises were used as resonators but coupled via quarter wavelength waveguide inverters [9], [10]. Recently, researchers also employed coupling irises as frequency-dependent coupling elements to generate transmission zeros (TZs) [11]. The novelty of our work is that the resonant iris not only facilitates the coupling to the adjacent cavity resonators but also work as a resonator, and no additional waveguide inverters is required. To the best of the authors' knowledge, this paper is the first report of a pole-generating resonant iris structure of this kind. Fig. 1 illustrates the internal structures of the proposed filter with proposed pole-generating resonant iris.

II. Resonant Iris

A. Concept of pole-generating resonant irises

Coupled cavity filters usually use irises (thin metallic diaphragms) to realize the coupling between cavities. From circuit point of view, the irises can be represented as shunt capacitance or inductance. In [9], [10], the capacitive and inductive irises were integrated together to implement a shunt resonator, but the coupling between them relies on extra quarter wavelength waveguide inverters. In this paper, we propose the pole-generating resonant iris, which can generate a TP as resonator without extra waveguide inverters required. The initial idea of this design comes from a common phenomenon, where the coupling irises often bring a spurious resonance above the passband, deteriorating the out-of-band rejection, especially for wideband filters. Fig. 2 presents the frequency response of such a filter with inductive irises and the TE_{101}-like electric field pattern of the iris resonance. To suppress this spurious resonance, one method is to move the iris resonance to higher frequency by dividing the single iris to multiple smaller aperture irises as proposed in [6]. In this work, instead of pushing the resonance away, we propose a method to take advantage of this iris resonance and use it in the filter design. We will present a novel resonant iris structure, which not only leverages the undesired iris resonance but also offers the capability to control the coupling between two resonators on either side of the iris. It is worth noting that although rectangular cavity resonators are used here as a demonstrator, the resonant iris concept could work with many other resonators.

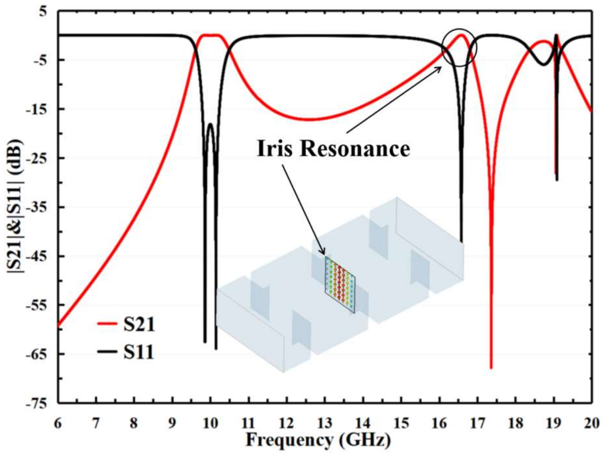

Fig. 2. Frequency response of a conventional two-pole coupled cavity filter using inductive irises, with inset showing the E-field pattern of the iris resonance projected on the middle cross-section.

B. Design of resonant iris

To demonstrate the pole-generating resonant iris concept, an L-shaped resonant iris is designed. As shown in Fig. 3(a), an extra metallic diaphragm was added next to the symmetric inductive iris. Since the added diaphragm introduces the discontinuity into the H-plane and E-plane simultaneously, a L-shaped resonant aperture is achieved. The L-shaped resonant aperture has a longer effective resonance wavelength than the classic rectangular resonant iris. Fig. 3(b) shows three key parameters and the simulated electric field distribution of the used resonance mode. The electric field pattern is like a folded TE_{101} mode, and the field distribution is folded and condensed. Hence the size of this resonant iris can be reduced at the cost of a lower unloaded quality. The miniature resonant iris can be inserted between two rectangular resonators and provides an iris resonance within the passband. It is also important to note that the coupling strength can be enhanced as the field can be coupled through the whole cross-section of the L-shape aperture. This enables wideband capability.

C. Coupling model of the resonant iris

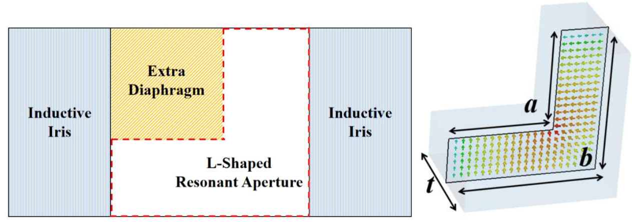

Fig. 3. Miniature pole-generating resonant iris. (a) Front view of the structure. (b) E-field pattern of its resonance mode projected on the E-plane.

Consider the filter model in Fig. 1(a), where the resonant iris is sandwiched between two TE_{101} resonators. The filter is fed by two WR-90 waveguides. This filter can be represented by the coupling scheme in Fig. 4(a). While the resonant iris provides the additional resonance node 2, it also allows the coupling k_{13} like the conventional coupling iris. So, it should behave like a singlet, which exhibits a reflection–transmission zero pair in the frequency response [12]. To verify the pole-generating feature, we deliberately make the external coupling weak and render the filter mismatched. From Fig. 4(b), it is clear that three transmission poles can be generated because of the resonant iris. Fig. 4(c) illustrates the wideband transmission response. As expected, the coupling k_{13}, working as a crossing coupling, provides a TZ for the third-order filter. When an extra coupling iris, controlling the k_{13}, is added as shown in the inset, the TZ can be reduced in frequency with almost no impact on the passband. This feature can be explored to improve the skirt selectivity.

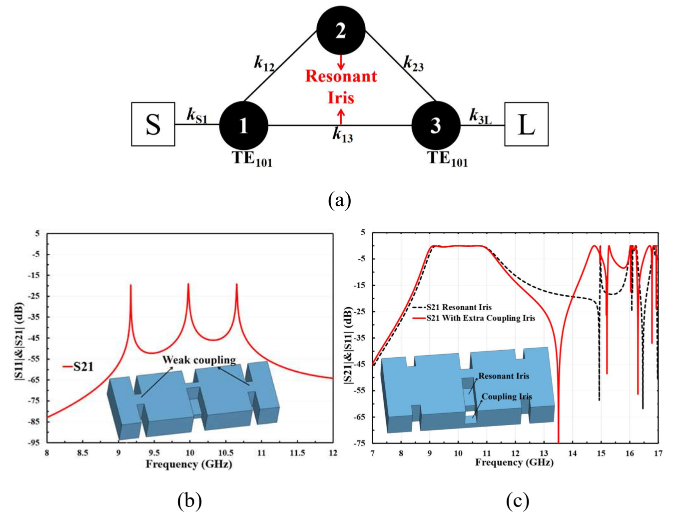

Fig. 4. (a) Coupling scheme of the filter in Fig. 1(a). (b) Frequency response of this filter when it is deliberately mismatched (see the inset). (c) Comparison between filter with and without extra coupling iris.

Extracting the coupling coefficient is a non-trivial step for this class of filter because there is no separable coupling structure as in conventional waveguide filters. Considering the asymmetry of the two coupled elements – the resonant iris and the waveguide cavity, we employ the S-parameter approach [13] to calculate the inter-resonator coupling. Fig. 5(a) shows the EM simulation model used for coupling extraction. Pins of two added SMA connectors are inserted

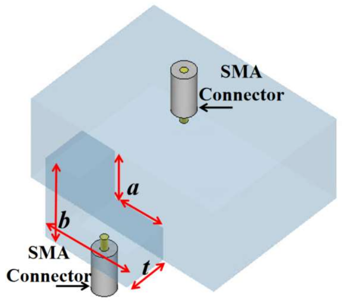

(a)

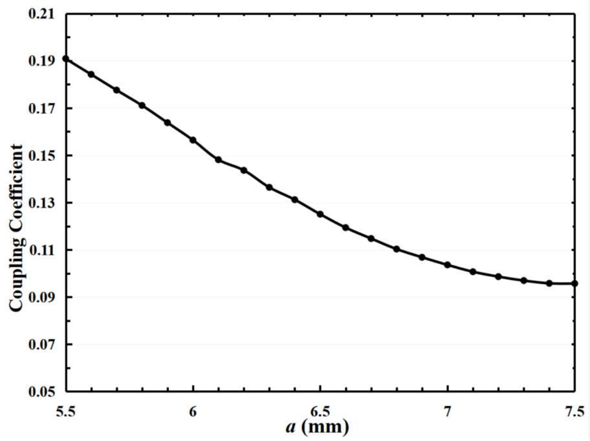

(b)

Fig. 5. (a) EM simulation model for inter-resonator coupling coefficient extraction. (b) Extracted coupling coefficient versus the dimensional parameter a.

into resonators to provide the weak coupling. Meanwhile, the open-circuit side of the resonant iris is approximated as a perfect magnetic wall to account for the loading effect from adjacent resonator. The coupling strength is mainly controlled by the dimensional parameter *a*. Fig. 5(b) presents the extracted coupling coefficient as a function of *a*. It is worth noting that although *a* could also affect the resonance frequency, it can be compensated by varying the dimensional parameter *b*. The parameter *t* can further assist with coupling tuning with little impact on the resonance frequency.

III. DESIGN EXAMPLES

A third-order X-band filter centered at 9 GHz, with the fractional bandwidth of 9.5%, has been adopted here as a design example. This filter is designed to have Chebyshev response with passband return loss of 20 dB. Its internal structure is like the one in Fig. 1. Fig. 6 compares the simulated filter performance and the ideal response from the coupling matrix. The nonzero elements of the normalized matrix are $k_{S1} = k_{3L} = 1.08$ and $k_{12} = k_{23} = 1.03$. As can be observed, the response of the initial design, after dimension extraction, is close to the ideal response. The response after optimization agrees well in the vicinity of the passband. This confirms the feasibility of applying coupling matrix model to the proposed resonant iris structures. In this case, the couplings between the resonant iris and the two resonators are the same. For higher order filters, the resonant iris can be

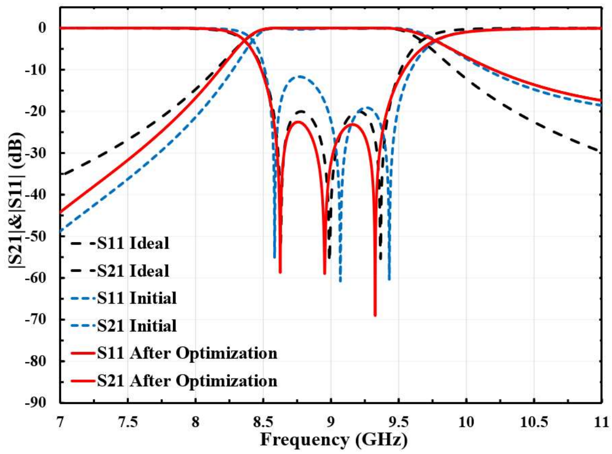

Fig. 6. Comparison of simulated filter performances: from extracted initial dimensions, after optimization, and from the ideal response determined by the coupling matrix.

re-designed for the required asymmetric coupling.

An evident benefit brought by this novel iris structure is the footprint reduction. The overall length of the filter can be reduced by 20% from that of a conventional third-order waveguide resonator filter. Fig. 7(a) shows a comparison. The out-of-band rejection is also significantly improved while the insertion loss is kept at a similar level. The simulated insertion loss is 0.067 dB for the traditional and 0.078 dB for the resonant iris filter when the conductor material is assumed to be aluminium. The slightly higher loss of the new filter is due to the lower Q of the resonation iris.

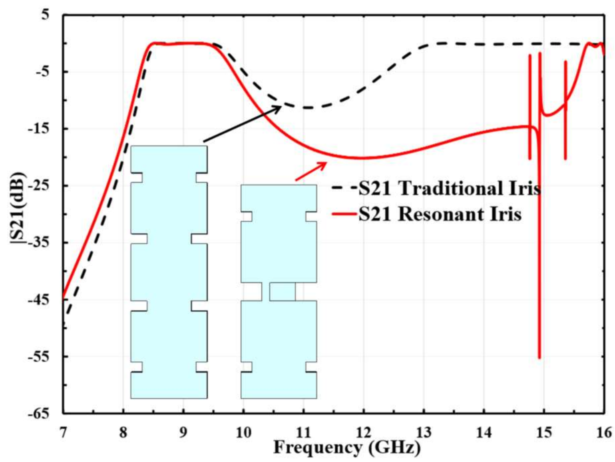

Fig. 7. Comparison between a traditional TE_{101} mode filter and the filter with resonant iris.

Finally, a prototype design was fabricated monolithically by selective laser melting (SLM) technique [14] using the twin-laser SLM500HL system and aluminum-copper-based alloy powder (A20X) at the University of Birmingham. Fig. 8 shows the CAD model used in 3D printing where the blue colour represents the supporting structure. The filter is oriented by 45° during the SLM printing. This avoids overhang structures insider the filter and therefore no internal supporting structure is needed.

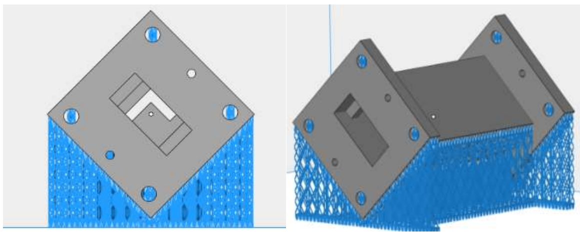

Fig. 8. Filter orientation and external support structure (indicated in blue) used in the SLM 3D printing.

Fig. 9 shows the measurement result and the photograph of the printed sample. The external dimensions of the sample are 54 mm × 32.86 mm × 20.16 mm excluding the connection flanges. No surface finishing treatment was used on this sample except at the two flange interfaces. The measured centre frequency and average insertion loss are 9.08 GHz and 0.15 dB respectively. Without any tuning, the measured response agrees very well with the simulation. The transmission poles have moved slightly. It is expected that tuning should improve this if required.

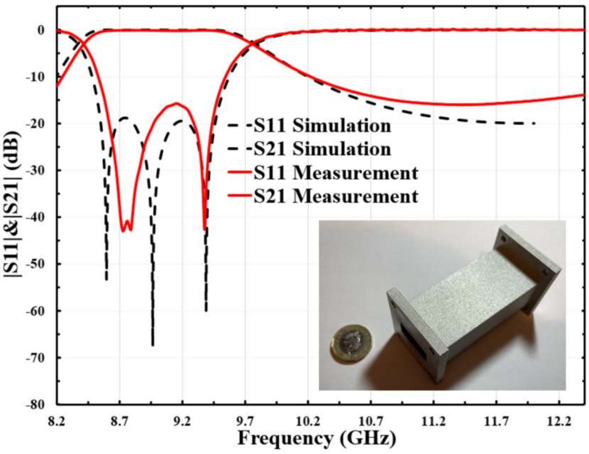

Fig. 9. Measured and simulated results of the design example with inset showing the photograph of the monolithically printed filter.

IV. Conclusion

In this paper, a novel pole-generating resonant iris structure was proposed for coupled cavity filters. By introducing the resonant iris, a filter with more compact footprint and improved out-of-band performance is achieved. A filter prototype has been subsequently implemented monolithically using SLM based metal 3D printing technology and experimentally verified, to demonstrate the feasibility of the proposed resonant iris concept.

References

[1] S. Wong, S. Member, S. Feng, S. Member, and L. Zhu, "Triple- and Quadruple-Mode Wideband Bandpass," *IEEE Trans. Microw. Theory Tech.*, vol. 63, no. 10, pp. 3416–3424, 2015.

[2] J. Jiang and R. R. Mansour, "Wideband dielectric substrate-loaded cavity filter," *IEEE Trans. Microw. Theory Tech.*, vol. 68, no. 1, pp. 111–120, 2020.

[3] B. Theron, S. Vigneron, and H. Baudrand, "A Two-Step Synthesis of Broadband Ridged Waveguide Bandpass Filters with Improved Performances," *IEEE Trans. Microw. Theory Tech.*, vol. 39, no. 12, pp. 2192–2197, 1991.

[4] Q. Zhang and Y. Lu, "Dimensional synthesis of symmetric wideband waveguide cross-coupled filters without global full-wave optimization," *IEEE Trans. Microw. Theory Tech.*, vol. 58, no. 12 PART 1, pp. 3742–3748, 2010.

[5] Z. Li, P. Zhao, and K. L. Wu, "An I/O coupling multiplier circuit and its application to wideband filters and diplexers," *IEEE Trans. Components, Packag. Manuf. Technol.*, vol. 8, no. 5, pp. 858–866, 2018.

[6] C. Tomassoni, M. Dionigi, and R. Sorrentino, "Strategies for the improvement of the out of band behavior of TM dual-mode filters," *2015 IEEE 1st Int. Forum Res. Technol. Soc. Ind. RTSI 2015 - Proc.*, pp. 90–93, 2015.

[7] S. F. Feng, S. W. Wong, L. Zhu, and Q. X. Chu, "A Triple-mode Wideband Bandpass Filter Using Single Rectangular Waveguide Cavity," *IEEE Microw. Wirel. Components Lett.*, vol. 27, no. 2, pp. 117–119, 2017.

[8] I. C. Hunter, L. Billonet, B. Jarry, and P. Guillon, "Microwave filters - Applications and technology," *IEEE Trans. Microw. Theory Tech.*, vol. 50, no. 3, pp. 794–805, 2002.

[9] [9] T. S. Chen, "Characteristics of Waveguide Resonant-Iris Filters," *IEEE Trans. Microw. Theory Tech.*, vol. 15, no. 4, pp. 260–262, Apr. 1967.

[10] M. Piloni, R. Ravenelli, and M. Guglielmi, "Resonant aperture filters in rectangular waveguide," in *1999 IEEE MTT-S International Microwave Symposium Digest (Cat. No.99CH36282)*, 1999, vol. 3, pp. 911–914.

[11] U. Rosenberg, S. Amari, and F. Seyfert, "Pseudo-elliptic direct-coupled resonator filters based on transmission-zero-generating irises," *Eur. Microw. Week 2010, EuMW2010 Connect. World, Conf. Proc. - Eur. Microw. Conf. EuMC 2010*, no. September, pp. 962–965, 2010.

[12] S. Bastioli, "Nonresonating mode waveguide filters," *IEEE Microw. Mag.*, vol. 12, no. 6, pp. 77–86, 2011.

[13] R. J. Cameron, C. M. Kudsia, and R. R. Mansour, *Microwave Filters for Communication Systems*. Hoboken, NJ, USA: John Wiley & Sons, Inc., 2018.

[14] I. Gibson, D. W. Rosen, and B. Stucker, *Additive Manufacturing Technologies*. Boston, MA: Springer US, 2010.